

V.I.

* . * . * . ** . ** . **

Parameter Study for the Analysis of Impact Characteristics considering Dynamic Material Properties

J.H. Lim, J.H. Song, H. Huh, W.J. Park, I.S. Oh, J.W. Choe

Key Words : Split Hopkinson pressure bar(), Vacuum interrupter(),
Strain rate hardening(), Chattering()

Abstract

Vacuum interrupters that is used in various switchgear components such as circuit breakers, distribution switches, contactors, etc. spreads the arc uniformly over the surface of the contacts. The electrode of vacuum interrupters is used sintered Cu-Cr material satisfied with good electrical and mechanical characteristics. Because the closing velocity is 1-3m/s, the deformation of the material of electrodes depends on the strain rate and the dynamic behavior of the sintered Cu-Cr material is a key to investigate the impact characteristics of the electrodes. The dynamic response of the material at the high strain-rate is obtained from the split Hopkinson pressure bar test using cylinder type specimens. Experimental results from both quasi-static and dynamic compressive tests with the split Hopkinson pressure bar apparatus are interpolated to construct the Johnson-Cook equation as the constitutive relation that should be applied to simulation of the dynamic behavior of electrodes. To evaluate impact characteristic of a vacuum interrupter, simulation is carried out with five parameters such as initial velocity, added mass of a movable electrode, wipe spring constant, initial offset of a wipe spring and virtual fixed spring constant.

1.

가 (vacuum interrupter)

가 가

V.I.

가

(electrode),

가

V.I. ms

(VCB; vacuum circuit breaker)

가

1 가

가

(chattering)

*

** LG

가

. VI.

2.2

Johnson, Cook

1/sec 1000/sec

=1/sec

Instron4206

ASTM E-8

가 20mm

. VI.

1/sec

Dynamic UTM

가

가 6mm

가 90mm

2.

2.1

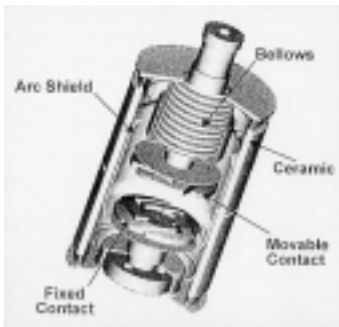


Fig. 1 Structure of a vacuum interrupter.

Fig.1

(fixed contact), 가 (movable contact),
(arc shield),
(bellows)

가

kV, kA

가

가

가

2 m/s

(bounce)

Fig.2



Fig. 2 Split Hopkinson pressure bar

(1) (2)

$$\sigma(t) = E \frac{A_0}{A} \varepsilon_T(t) \quad (1)$$

$$\dot{\varepsilon}(t) = -\frac{2C_0}{L} \varepsilon_R(t) \quad (2)$$

Johnson-Cook

log

가 1/sec

(normalize)

$$\bar{\sigma} = [A + B\bar{\varepsilon}^n][1 + C \ln \bar{\dot{\varepsilon}}][1 - T^{3m}] \quad (2-13)$$

$$T^* = \frac{T - T_{room}}{T_{melt} - T_{room}} \quad (2-14)$$

T_{room} T_{melt}
 27°C 1500/sec
 가 가 가 가

가

가

가

90%가

Johnson-Cook

Fig.3

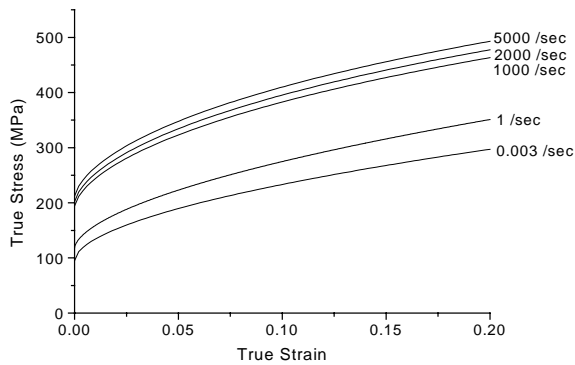


Fig. 3 Fitted stress-strain curve of sintered Cu-Cr.

3.

3.1

V.I.

LS-DYNA3D

3:1

8518kg/m³,

396J/kgK

8960kg/m³,

383J/kgK

Fig.4

10844

14836

가

가

(wipe spring)

Fig.4

30.8mm

118.5 N/mm

가 5.5mm 가

가 1~1.5m/s

1.2m/s

Fig.5

가

. #1

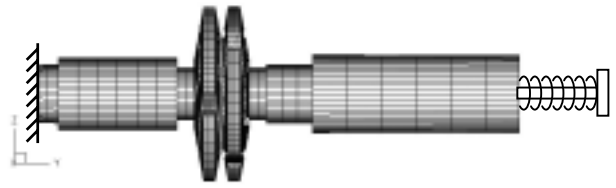


Fig. 4 The finite element model of a vacuum interrupter.

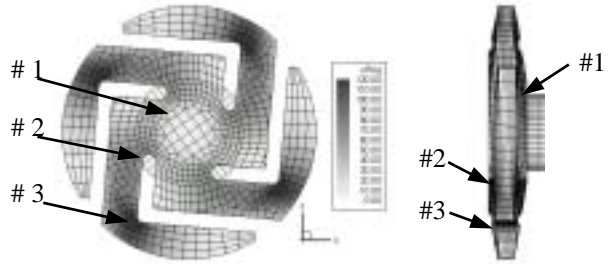


Fig. 5 Three points with the largest effective stress: (a) front view; (b) side view.

, #2

가

, #3

가

가

, 가

가

가

가

가

3.2 가

Fig.6 가

가 1.0-

1.5m/s

m/s

1.0, 1.2, 1.5, 1.8, 2.5

가 가

가 가

가

#2

가

가

#3

가

Fig.7

가 가 가

가 가

가

가 가 가

가

가

가

가

#3

Fig.8

가

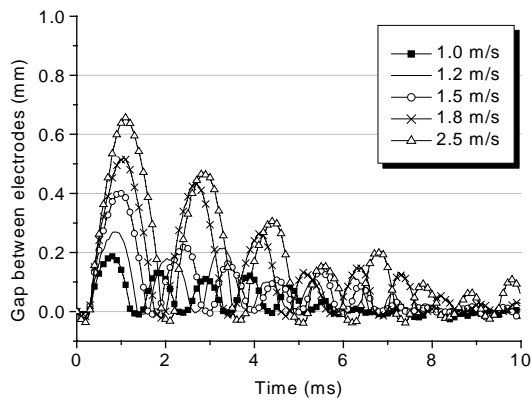


Fig. 6 The distance between the fixed and the movable electrodes with velocity of the movable electrode.

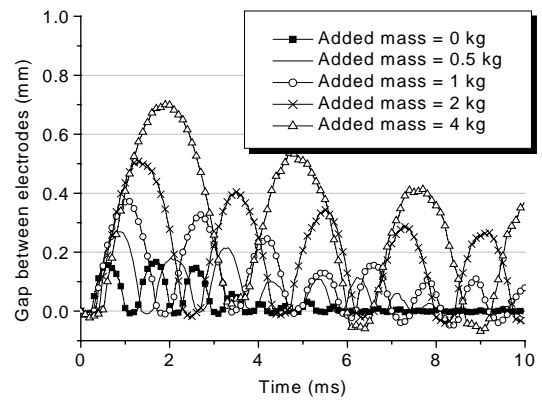


Fig. 9 The distance between the fixed and the movable electrodes with added movable mass

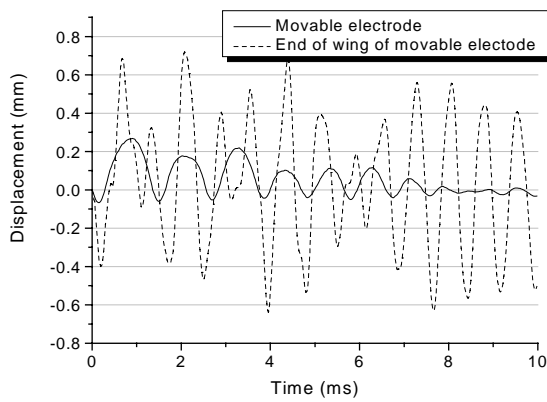


Fig. 7 Displacements of a movable electrode and the end of wing of a movable electrode.

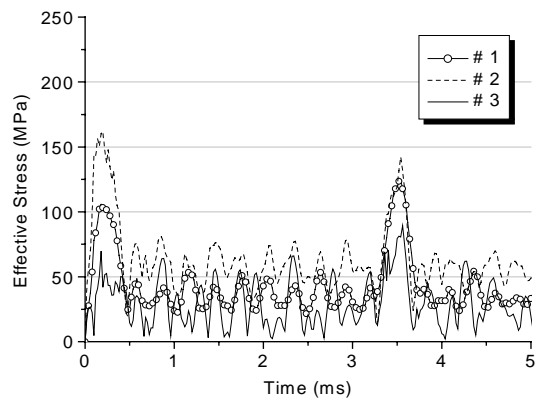


Fig. 10 The effective stress versus time graph of the movable electrode with added mass = 4kg.

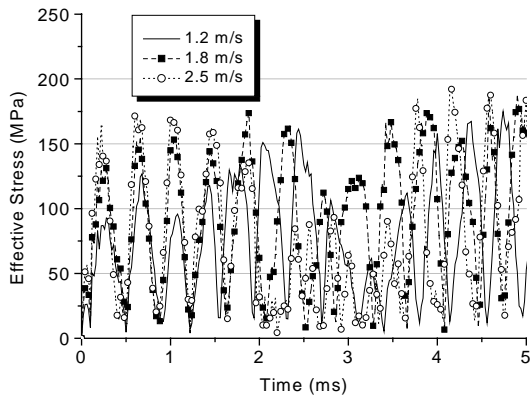


Fig. 8 The effective stress of #3 for the movable electrode with velocity of the movable electrode.

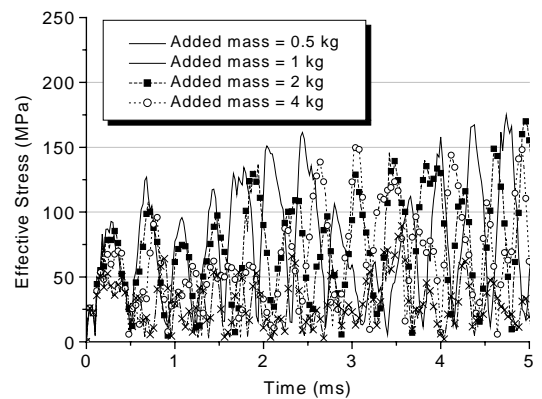


Fig. 11 The effective stress of #3 for the movable electrode with added movable mass.

가 가 #2 , 가
 #3
 3.3 가 가
 Fig.9 가 가
 가 0, 0.5, 1, 2,
 4kg 가

가
 가 Fig.10
 가 4kg 가
 가 0.5kg #3
 가 4kg #2
 가 가 가
 가 #3 #2
 Fig.11 가 #3

0kg, 0.5kg, 1kg 가 #3
 #2 4kg 가
 #2 가 가 #3
 가 가 가 #2
 , 가 가
 3.4 Fig.12 가

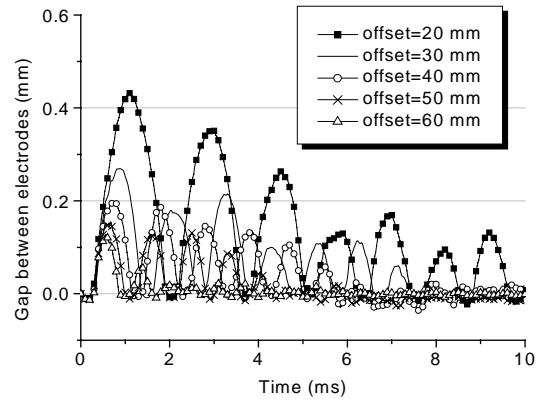


Fig. 14 The distance between the fixed and the movable electrodes with the initial offset of the wipe spring.

가 가
 가 가 Fig.13 가
 #3 가 가
 가 가
 3.5 Fig.14 가
 가

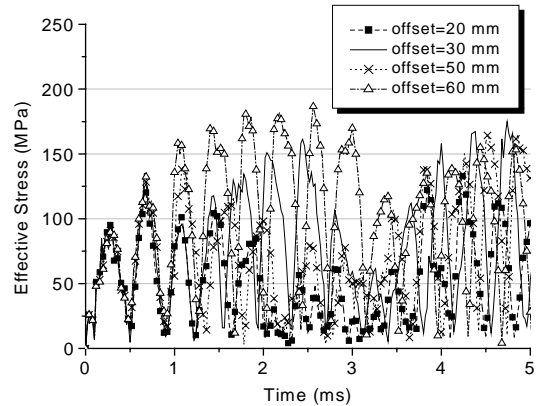


Fig. 15 The effective stress of #3 for the movable electrode with initial offset of the wipe spring.

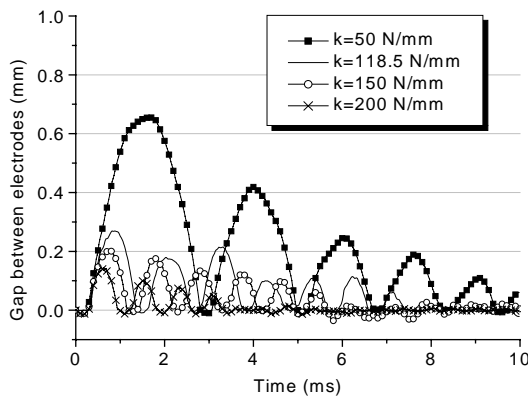


Fig. 12 The distance between the fixed and the movable electrodes with the wipe spring constant.

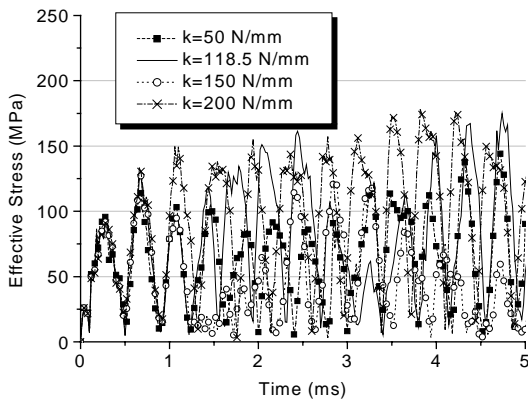


Fig. 13 The effective stress of #3 for the movable electrode with the wipe spring constant.

가 가
 가 Fig.15
 3.6 가
 가 가
 가 가
 Fig.16 가 10, 20, 100, 1000
 kN/mm 가 20kN/mm
 100IN/mm

